

ON THE DUALITY OF THE POTENTIAL METHOD AND THE POINT SOURCE METHOD IN INVERSE SCATTERING PROBLEMS

JIJUN LIU AND ROLAND POTTHAST

Communicated by Charles Groetsch

*This paper is dedicated to Prof. Dr. Rainer Kress
on the occasion of his 65th birthday.*

ABSTRACT. The reconstruction of scattered wave from its far-field pattern is of great importance in inverse scattering problems. The classic *potential method* due to Kirsch and Kress is a well known scheme by solving an integral equation of the first kind with respect to a density function, which relates the scattered wave to its far-field pattern. In recent years, a filtering scheme known as *point source method*, is also well developed, which is based on the point source decomposition and the reciprocity principle. This paper aims to consider the *quantitative relation* between these two regularizing methods. We prove that these two schemes will generate *exactly the same approximate solution* when used with identical geometric setup and if their own regularizing parameters are taken as a constant multiple (a *golden rule*). Our key step is to employ an *adjoint relation* between the Herglotz wave operator and the far-field operator. Further we provide estimates of the solutions with regularization parameters different from the golden rule. As illustration and for practical testing of these results numerical examples are presented to show the numerical equivalence of these two methods.

1. Introduction. Inverse problems for acoustic and electromagnetic waves play an important role in many scientific and engineering applications. One of the important topics in this area is the reconstruction of scattered wave outside of the scatterer D from its far-field pattern. The well known Rellich lemma guarantees the unique deter-

Keywords and phrases. Inverse scattering, potential theory, point source method, duality, regularization, numerics.

Received by the editors on September 26, 2007, and in revised form on March 26, 2008.

DOI:10.1216/JIE-2009-21-2-297 Copyright ©2009 Rocky Mountain Mathematics Consortium

mination of the scattered wave theoretically, while the practical motivation of these kinds of problems come from the following three facts. Firstly, the far-field pattern $u^\infty(\hat{x})$ is relatively easy to measure in the applied area. The reconstruction scheme enables the determination of the scattered wave in a unbounded domain $\mathbb{R}^m \setminus \overline{D}$ from the measured data of $u^\infty(\hat{x})$ specified in the unit sphere $\mathbb{S}^{m-1} \in \mathbb{R}^m$. Secondly, when the zero-curve set method of the scattered wave is used to reconstruct the obstacle shape based on the optimization and iteration techniques, compare [4], the scattered wave must be evaluated from its far field pattern. Finally, for some recently developed obstacle shape reconstruction schemes such as probe method and singular sources method from the far-field pattern, see [1, 2, 3, 12, 13], the key to the reconstruction procedure is the transformation of the far-field data into the near field.

Therefore, some scattered wave reconstruction methods from its far field pattern have been developed, among which we would like to mention potential method, point source method and series method, see [4, 5, 7].

In our previous paper [8], we establish a relation between the potential method and point source method, which states that the point source method can be derived from via a classic potential approach. This generalizes the applicable area of point source method from incident plane wave to arbitrary incident wave. On the other hand, both of these methods reconstruct the scattered wave by solving an ill-posed integral equation of the first kind with respect to a density function. The *comparison of the degree of ill-posedness* for these two methods is quite important for the investigation and development of stable inversion schemes.

This paper aims to compare these two methods from the *quantitative* point of view. We prove that these two methods are *equivalent* or even *identical*: if the geometrical setting is chosen identically and if the regularizing parameter for one scheme is chosen as a constant multiple of that for the other scheme, then these two schemes will yield the exactly same solution! We denote this choice of regularization parameters as *golden rule*. The specified constant is linked to the fundamental solution to the Helmholtz equation. The key to this essential relation is the adjoint relation between the Herglotz wave operator \mathbb{H} and the far-field operator \mathbb{F} , which can be explained as a *duality relation* of the

two schemes. Further, we study the situation where the regularization parameters are not chosen according to the golden rule and provide error estimates. Finally, as illustration and confirmation of the results a numerical comparison of the field reconstructions is presented.

This paper is organized as follows. In Section 2, we give an outline for both potential method and point source method, which provide the basis for our comparison. Then we establish the duality and identity results for the two methods for suitably chosen regularizing parameters in Section 3. Finally in Section 4 we present some numerical results to compare the reconstruction performance by these two methods, where the "golden rule" for the regularizing parameters of these two schemes is supported numerically.

2. Potential method and point source method. In this section we describe the basic ideas of the Kirsch-Kress potential method and Potthast's point source method. This provides the framework for our further duality analysis of the two schemes.

Denote by $\Phi(x, y)$ the fundamental solution to the Helmholtz equation $\Delta u + \kappa^2 u = 0$ in \mathbb{R}^m with $m = 2, 3$, that is,

$$(1) \quad \Phi(x, y) = \begin{cases} \frac{i}{4} H_0^{(1)}(\kappa|x - y|), & m = 2 \\ \frac{e^{i\kappa|x - y|}}{4\pi|x - y|}, & m = 3 \end{cases}$$

and introduce

$$(2) \quad \gamma_2 = \frac{e^{i\frac{\pi}{4}}}{\sqrt{8\pi\kappa}}, \quad \gamma_3 = \frac{1}{4\pi}$$

in two or three dimensions, respectively.

For given incident wave $u^i(x)$, it is well known that the scattered wave $u^s(x)$ has the following asymptotic behavior

$$(3) \quad u^s(x) = \frac{e^{i\kappa|x|}}{|x|^{\frac{m-1}{2}}} \left(u^\infty(\hat{x}) + O\left(\frac{1}{|x|}\right) \right), \quad |x| \rightarrow \infty,$$

which comes from the Green representation formula of the scattered wave $u^s(x)$ and the asymptotic of $\Phi(x, y)$. One of the research topic in

inverse scattering problems is the reconstruction of $u^s(x)$ outside of D from its far-field pattern $u^\infty(\hat{x})$.

Assume that either

- (a) $\overline{D} \subset\subset G$ or more general
- (b) u^s can be analytically extended up to $\mathbb{R}^m \setminus G$.

Our goal is to compute the scattered wave in the domain $\mathbb{R}^m \setminus \overline{G}$ from its far-field pattern. Conditions (a) and (b) guarantee the solvability of this problem. Further, we assume that the homogeneous interior Dirichlet problem for the test domain G does have only the trivial solution. Since we can choose G , this condition does not restrict the applicability of the methods.

We firstly state the computational schemes of the point source method with a derivation according to Liu and Potthast and the potential method due to Kirsch and Kress as the following two algorithms. The algorithm for the point source method stated here is based on the derivation procedure given in [8].

Algorithm 2.1. (Point source method). The point source method reconstructs the scattered wave $u^s(x)$ in $\mathbb{R}^m \setminus \overline{G}$ using the following steps.

1. Approximate the point source $\Phi(\cdot, x)$ for any fixed $x \in \mathbb{R}^m \setminus \overline{G}$ by a superposition of plane waves by approximately solving the equation

$$(4) \quad \Phi(z, x) = \int_{\mathbb{S}^{m-1}} e^{i\kappa z \cdot d} g_x(d) ds(d), \quad z \in \partial G.$$

2. Then, the scattered field $u^s(x)$ can be calculated by evaluating the integral

$$(5) \quad u^s(x) = \frac{1}{\gamma_m} \int_{\mathbb{S}^{m-1}} u^\infty(-d) g_x(d) ds(d), \quad x \in \mathbb{R}^m \setminus \overline{G},$$

which is a kind of filtered reconstruction with filter function g_x .

Remark. We denote the integral in (4) by

$$(6) \quad \mathbb{H}[g_x](z) := \int_{\mathbb{S}^{m-1}} e^{i\kappa z \cdot d} g_x(d) ds(d), \quad z \in \partial G.$$

The operator \mathbb{H} is called the Herglotz wave operator. The derivation of the point source method can be carried out as follows. We express $u^s(x)$ outside of \overline{G} as well as its far-field pattern in terms of a single-layer approach with density ρ by

$$(7) \quad u^s(x) = \int_{\partial G} \Phi(z, x)\rho(z)ds(z), \quad x \in \mathbb{R}^m \setminus \overline{G},$$

$$(8) \quad u^\infty(\hat{x}) = \gamma_m \int_{\partial G} e^{-i\kappa\hat{x}\cdot z} \rho(z)ds(z), \quad \hat{x} \in \mathbb{S}^{m-1},$$

where the constant γ_m is defined in (2). By inserting (4) into (7) and exchanging the order of integration, we obtain (5). \square

The equation (4) for constructing the filter g_x may not have an exact solution. So it must be solved by regularization technique to get an approximate solution g_x^α such that (4) holds approximately. Then $u_\alpha^s(x)$ generated from (5) in terms of g_x^α gives an approximation to $u^s(x)$, that is,

$$(9) \quad u_\alpha^s(x) = \frac{1}{\gamma_m} \int_{\mathbb{S}^{m-1}} u^\infty(-d)[(\alpha I + \mathbb{H}^*\mathbb{H})^{-1}\mathbb{H}^*\Phi(\cdot, x)](d)ds(d), \\ x \in \mathbb{R}^m \setminus \overline{G},$$

where α is the regularizing parameter for this ill-posed problem. This is a concise form for the point source method for reconstructing the scattered wave from its far field pattern.

Algorithm 2.2. (The potential method). This classic method reconstructs the scattered wave, which is denoted by a different notation $v^s(x)$ for comparison, from the far-field pattern $v^\infty(\hat{x})$ by the following steps. As a preparation we note that we can express the scattered wave $v^s(x)$ outside of \overline{G} as well as its far-field pattern in terms of a single-layer approach with density ω , i.e.

$$(10) \quad v^s(x) = \int_{\partial G} \Phi(z, x)\omega(z)ds(z), \quad x \in \mathbb{R}^m \setminus \overline{G},$$

$$(11) \quad u^\infty(\hat{x}) = \gamma_m \int_{\partial G} e^{-i\kappa\hat{x}\cdot z} \omega(z) ds(z), \quad \hat{x} \in \mathbb{S}^{m-1},$$

where $\mathbb{F} : L^2(\partial G) \rightarrow L^2(\mathbb{S}^{m-1})$ defined by

$$(12) \quad \mathbb{F}[\omega](\hat{x}) := \gamma_m \int_{\partial G} e^{-i\kappa\hat{x}\cdot z} \omega(z) ds(z), \quad \hat{x} \in \mathbb{S}^{m-1},$$

is called the far-field operator.

1. Solve the density function $\omega(z)$ from (11) by regularizing scheme

$$(13) \quad \omega_\beta(z) = [(\beta I + \mathbb{F}^* \mathbb{F})^{-1} \mathbb{F}^* u^\infty](z)$$

with a specified regularizing parameter $\beta > 0$.

2. Insert the density function into (10) to generate

$$(14) \quad v_\beta^s(x) = \int_{\partial G} \Phi(z, x) [(\beta I + \mathbb{F}^* \mathbb{F})^{-1} \mathbb{F}^* u^\infty](z) ds(z), \quad x \in \mathbb{R}^m \setminus \overline{G}$$

as an approximation to the scattered wave.

Denote by $\{\varphi_j, \psi_j, \mu_j\}_{j \in \mathbb{N}}$ the singular system of compact operator \mathbb{H} from the Hilbert space $L^2(\mathbb{S}^{m-1})$ to $L^2(\partial G)$, that is,

$$(15) \quad \mathbb{H}\varphi_j = \mu_j \psi_j, \quad \mathbb{H}^* \psi_j = \mu_j \varphi_j, \quad j = 1, 2, \dots$$

It is easy to verify that

$$(16) \quad \mathbb{F}^* = \overline{\gamma}_m \mathbb{H}, \quad \mathbb{F} = \gamma_m \mathbb{H}^*$$

in the dual system $(L^2(\mathbb{S}^{m-1}), L^2(\partial G))$ with the complex inner product in $L^2(\mathbb{S}^{m-1})$ and $L^2(\partial G)$ respectively, that is,

$$(17) \quad \begin{aligned} \langle \overline{\gamma}_m \mathbb{H}\varphi, \psi \rangle_{L^2(\partial G)} &= \langle \varphi, \mathbb{F}\psi \rangle_{L^2(\mathbb{S}^{m-1})}, \\ \langle \varphi, \gamma_m \mathbb{H}^* \psi \rangle_{L^2(\mathbb{S}^{m-1})} &= \langle \mathbb{F}^* \varphi, \psi \rangle_{L^2(\partial G)}, \end{aligned}$$

where

$$\begin{aligned} \langle \tilde{\varphi}, \varphi \rangle_{L^2(\mathbb{S}^{m-1})} &:= \int_{\mathbb{S}^{m-1}} \tilde{\varphi}(d) \overline{\varphi(d)} ds(d), \\ \langle \tilde{\psi}, \psi \rangle_{L^2(\partial G)} &:= \int_{\partial G} \tilde{\psi}(z) \overline{\psi(z)} ds(z) \end{aligned}$$

for all complex value functions $\tilde{\varphi}, \varphi \in L^2(\mathbb{S}^{m-1})$ and $\tilde{\psi}, \psi \in L^2(\partial G)$, where \bar{w} represents the complex conjugate of w .

Under the above analysis, it can be seen from (9, 14 and 16) that the point source method and potential method are *dual* to each other with respect to the dual system $\langle L^2(\mathbb{S}^{m-1}), L^2(\partial G) \rangle$. Here, we work out a precise form of this duality and show quantitative relations between these two schemes.

3. Quantitative relation between two schemes . The central result of this section shows identity of the field reconstructions of the Kirsch-Kress potential method and Potthast's point source method. We firstly give a lemma proving properties of the singular system of \mathbb{H} , which is our basis for establishing the duality and revealing the quantitative relation of these two reconstruction schemes.

Lemma 3.1. *For any $l, j \in \mathbb{N}$, the singular system of \mathbb{H} has the following property.*

1. *If $\mu_l = \mu_j$, then*

$$(18) \quad \langle \varphi_l(-\cdot), \overline{\varphi_j(\cdot)} \rangle_{L^2(\mathbb{S}^{m-1})} = \langle \psi_l, \overline{\psi_j} \rangle_{L^2(\partial G)}.$$

2. *If $\mu_l \neq \mu_j$, then*

$$(19) \quad \langle \varphi_l(-\cdot), \overline{\varphi_j(\cdot)} \rangle_{L^2(\mathbb{S}^{m-1})} = \langle \psi_l, \overline{\psi_j} \rangle_{L^2(\partial G)} = 0.$$

Proof. Using the definitions of inner product and singular system, it follows by exchanging the order of integration in \mathbb{S}^{m-1} and ∂G that

$$(20) \quad \begin{aligned} \langle \varphi_l(-\cdot), \overline{\varphi_j(\cdot)} \rangle_{L^2(\mathbb{S}^{m-1})} &= \frac{1}{\mu_j} \int_{\mathbb{S}^{m-1}} \varphi_l(-d) (\mathbb{H}^* \psi_j)(d) ds(d) \\ &= \frac{1}{\mu_j} \int_{\partial G} \psi_j(z) \int_{\mathbb{S}^{m-1}} e^{-i\kappa d \cdot z} \varphi_l(-d) ds(d) ds(z) \\ &= \frac{1}{\mu_j} \int_{\partial G} \psi_j(z) (\mathbb{H} \varphi_l)(z) ds(z) \\ &= \frac{\mu_l}{\mu_j} \langle \psi_l, \overline{\psi_j} \rangle_{L^2(\partial G)}. \end{aligned}$$

Therefore we have proven (18). On the other hand, we have that

$$\begin{aligned}
 (21) \quad \langle \varphi_l(-\cdot), \overline{\varphi_j(\cdot)} \rangle_{L^2(\mathbb{S}^{m-1})} &= \int_{\mathbb{S}^{m-1}} \varphi_l(-d) \varphi_j(d) ds(d) \\
 &= \int_{\mathbb{S}^{m-1}} \varphi_l(d) \varphi_j(-d) ds(d) \\
 &= \langle \varphi_j(-\cdot), \overline{\varphi_l(\cdot)} \rangle_{L^2(\mathbb{S}^{m-1})},
 \end{aligned}$$

which generates by using (20) again that

$$\begin{aligned}
 (22) \quad \langle \varphi_l(-\cdot), \overline{\varphi_j(\cdot)} \rangle_{L^2(\mathbb{S}^{m-1})} &= \langle \varphi_j(-\cdot), \overline{\varphi_l(\cdot)} \rangle_{L^2(\mathbb{S}^{m-1})} \\
 &= \frac{\mu_j}{\mu_l} \langle \psi_j, \overline{\psi_l} \rangle_{L^2(\partial G)} \\
 &= \frac{\mu_j}{\mu_l} \langle \psi_l, \overline{\psi_j} \rangle_{L^2(\partial G)}.
 \end{aligned}$$

Inserting this relation into (20) says

$$\frac{\mu_l^2 - \mu_j^2}{\mu_l \mu_j} \langle \psi_l, \overline{\psi_j} \rangle_{L^2(\partial G)} = 0.$$

So we get for $\mu_l \neq \mu_j$ that $\langle \psi_l, \overline{\psi_j} \rangle_{L^2(\partial G)} = 0$ and therefore $\langle \varphi_l(-\cdot), \overline{\varphi_j(\cdot)} \rangle_{L^2(\mathbb{S}^{m-1})} = 0$ from (22). The proof is complete. \square

Remark 3.2. From the standard result for the singular system of compact operator, it follows the orthogonal relation that

$$\langle \psi_l, \psi_j \rangle_{L^2(\partial G)} = \delta_{l,j}, \quad l, j \in \mathbb{N}.$$

Generally we do not have $\langle \psi_l, \overline{\psi_j} \rangle_{L^2(\partial G)} = \delta_{l,j}$. Our result $\langle \psi_l, \overline{\psi_j} \rangle_{L^2(\partial G)} = 0$ for $\mu_l \neq \mu_j$ comes from the relation (22), which is due to the special structure of operator \mathbb{H} .

Now let us establish the identity of reconstructions for the two schemes of reconstructing the scattered wave, namely, point source method and potential method. We will show that $u_\alpha^s(x)$ and $v_\beta^s(x)$ are exactly the same in the case of identical geometrical setup and regularizing parameters α, β chosen in a suitable multiple relation.

Theorem 3.3. *Assume that $u_\alpha^s(x)$ and $v_\beta^s(x)$ are constructed by the above two regularizing schemes from the same far-field pattern $u^\infty(\hat{x})$, respectively. If we take $\beta = \gamma_m \bar{\gamma}_m \alpha$, then it follows for all $x \in \mathbb{R}^m \setminus \bar{G}$ that*

$$(23) \quad u_\alpha^s(x) = v_\beta^s(x).$$

Proof. As a preparation we remark that under the assumptions on G stated above both \mathbb{H} and \mathbb{H}^* are injective, compare [11]. The theorem is equivalent to proving that

$$(24) \quad \int_{\mathbb{S}^{m-1}} u^\infty(-d)[(\alpha I + \mathbb{H}^* \mathbb{H})^{-1} \mathbb{H}^* \Phi(\cdot, x)](d) ds(d) \\ = \gamma_m \int_{\partial G} \Phi(z, x)[(\beta I + \mathbb{F}^* \mathbb{F})^{-1} \mathbb{F}^* u^\infty](z) ds(z)$$

for $\beta = \bar{\gamma}_m \gamma_m \alpha$ with the expressions taken from the reconstruction procedures of these two schemes.

Define $\varphi(d) := u^\infty(d) \in L^2(\mathbb{S}^{m-1})$ and $\psi(z) := \Phi(z, x) \in L^2(\partial G)$ for the simplicity of notations. Then the left-hand side L of (24) can be written as

$$(25) \quad \text{L} = \int_{\mathbb{S}^{m-1}} \varphi(-d)[(\alpha I + \mathbb{H}^* \mathbb{H})^{-1} \mathbb{H}^* \psi](d) ds(d),$$

while the right-hand side R of (24) for $\beta = \bar{\gamma}_m \gamma_m \alpha$ is

$$(26) \quad \text{R} = \gamma_m \int_{\partial G} \psi(z)[(\beta I + \mathbb{F}^* \mathbb{F})^{-1} \mathbb{F}^* \varphi](z) ds(z) \\ = \gamma_m \bar{\gamma}_m \int_{\partial G} \psi(z)[(\beta I + \bar{\gamma}_m \gamma_m \mathbb{H} \mathbb{H}^*)^{-1} \mathbb{H} \varphi](z) ds(z) \\ = \int_{\partial G} \psi(z)[(\alpha I + \mathbb{H} \mathbb{H}^*)^{-1} \mathbb{H} \varphi](z) ds(z)$$

in terms of (16). The standard expansion theorem for the regularizing equation yields for all $\alpha > 0$ that

$$(27) \quad \left\{ \begin{array}{l} [(\alpha I + \mathbb{H}^* \mathbb{H})^{-1} \mathbb{H}^* \psi](d) = \sum_{j \in \mathbb{N}} \frac{\mu_j}{\alpha + \mu_j^2} \langle \psi, \psi_j \rangle_{L^2(\partial G)} \varphi_j(d), \\ [(\alpha I + \mathbb{H} \mathbb{H}^*)^{-1} \mathbb{H} \varphi](z) = \sum_{l \in \mathbb{N}} \frac{\mu_l}{\alpha + \mu_l^2} \langle \varphi, \varphi_l \rangle_{L^2(\mathbb{S}^{m-1})} \psi_l(z). \end{array} \right.$$

On the other hand, since both \mathbb{H} and \mathbb{H}^* are injective, we can expand φ, ψ in terms of φ_l, ψ_l as

$$(28) \quad \begin{aligned} \varphi(-d) &= \sum_{l \in \mathbb{N}} \langle \varphi, \varphi_l \rangle_{L^2(\mathbb{S}^{m-1})} \varphi_l(-d), \\ \psi(z) &= \sum_{j \in \mathbb{N}} \langle \psi, \psi_j \rangle_{L^2(\partial G)} \psi_j(z). \end{aligned}$$

Now we insert (28) and (27) into (25) and (26), respectively, to get

$$(29) \quad \begin{aligned} \mathbb{L} &= \sum_{j \in \mathbb{N}} \frac{\mu_j}{\alpha + \mu_j^2} \langle \psi, \psi_j \rangle_{L^2(\partial G)} \sum_{l \in \mathbb{N}} \langle \varphi, \varphi_l \rangle_{L^2(\mathbb{S}^{m-1})} \langle \varphi_l(-\cdot), \overline{\varphi_j(\cdot)} \rangle_{L^2(\mathbb{S}^{m-1})} \\ &= \sum_{j, l \in \mathbb{N}} \frac{\mu_l}{\alpha + \mu_j^2} \langle \psi, \psi_j \rangle_{L^2(\partial G)} \langle \varphi, \varphi_l \rangle_{L^2(\mathbb{S}^{m-1})} \langle \psi_l, \overline{\psi_j} \rangle_{L^2(\partial G)} \end{aligned}$$

from Lemma 3.1 and

$$(30) \quad \mathbb{R} = \sum_{j, l \in \mathbb{N}} \frac{\mu_l}{\alpha + \mu_l^2} \langle \psi, \psi_j \rangle_{L^2(\partial G)} \langle \varphi, \varphi_l \rangle_{L^2(\mathbb{S}^{m-1})} \langle \psi_l, \overline{\psi_j} \rangle_{L^2(\partial G)}.$$

In the case where $\mu_l = \mu_j$ by trivial equality and in the case where $\mu_l \neq \mu_j$ by Lemma 3.1 we obtain

$$\frac{\mu_l}{\alpha + \mu_j^2} \langle \psi, \psi_j \rangle_{L^2(\partial G)} \langle \varphi, \varphi_l \rangle_{L^2(\mathbb{S}^{m-1})} \langle \psi_l, \overline{\psi_j} \rangle_{L^2(\partial G)} = \frac{\mu_l}{\alpha + \mu_l^2} \langle \psi, \psi_j \rangle_{L^2(\partial G)} \langle \varphi, \varphi_l \rangle_{L^2(\mathbb{S}^{m-1})} \langle \psi_l, \overline{\psi_j} \rangle_{L^2(\partial G)} = 0.$$

That is, for any fixed pairs (l, j) , the corresponding terms in the summation of left-hand side and right-hand side are the same. So both sides has the same series expression

$$\mathbb{L} = \mathbb{R} = \sum_{(j, l) \in \mathbb{N}^2 \cap \{(j, l) : \mu_l = \mu_j\}} \frac{\mu_l}{\alpha + \mu_l^2} \langle \psi, \psi_j \rangle_{L^2(\partial G)} \langle \varphi, \varphi_l \rangle_{L^2(\mathbb{S}^{m-1})} \langle \psi_l, \overline{\psi_j} \rangle_{L^2(\partial G)},$$

noticing that $\langle \psi_l, \overline{\psi_j} \rangle_{L^2(\partial G)} = 0$ for $\mu_l \neq \mu_j$. This series is obviously convergent, since both sides of (24) are convergent as integrals for continuous integrands. The proof is complete. \square

Remark 3.4. We call the relation $\beta = \overline{\gamma}_m \gamma_m \alpha$ the *golden rule* for matching the potential method and point-source method, since the

two different schemes generate exactly the same reconstruction result for their regularizing parameters coupled in this exact relation. Such a *golden rule* is the quantitative representation of duality relation between point source method and potential method.

Next we want to consider the difference between $u_\alpha^s(x) - v_\beta^s(x)$, if the regularizing parameters of these two schemes do not match this golden rule. This can be built on the continuity of the regularization schemes with respect to the regularization parameter α or β , respectively. We will use two arbitrary regularization parameters α, β and also consider the special case where

$$(31) \quad \beta = K\tilde{\beta}, \quad \tilde{\beta} := \bar{\gamma}_m \gamma_m \alpha$$

with the ratio number $K > 0$.

Theorem 3.5. *For arbitrary regularizing parameters $\alpha, \beta > 0$ and $\tilde{\beta} := \bar{\gamma}_m \gamma_m \alpha$ we have*

$$(32) \quad \|u_\alpha^s(x) - v_\beta^s(x)\| \leq C \frac{|\beta - \tilde{\beta}|}{\tilde{\beta}}$$

with some constant $C = C(x)$. If $\beta = K\bar{\gamma}_m \gamma_m \alpha$ with some constant $0 < K \neq 1$, it holds that

$$(33) \quad \|u_\alpha^s(x) - v_\beta^s(x)\| \leq \frac{|K-1|}{K} \omega(K, \alpha), \quad x \in \mathbb{R}^m \setminus \bar{G},$$

with some function $\omega(K, \alpha)$ which satisfies $\omega(K, \alpha) \rightarrow 0$ as $\alpha \rightarrow 0$ for any fixed number $K > 0$.

Proof. For the first part we estimate

$$(34) \quad \begin{aligned} |u_\alpha^s(x) - v_\beta^s(x)| &\leq |u_\alpha^s(x) - v_{\tilde{\beta}}^s(x)| + |v_{\tilde{\beta}}^s(x) - v_\beta^s(x)| \\ &= |v_{\tilde{\beta}}^s(x) - v_\beta^s(x)|. \end{aligned}$$

We use the representation (10) via a single-layer potential with density ω_β to estimate

$$(35) \quad |v_{\tilde{\beta}}^s(x) - v_\beta^s(x)| \leq C \|\omega_{\tilde{\beta}}(x) - \omega_\beta(x)\|$$

with some constant C depending on G and x . For the estimate of the right-hand side we employ the arguments of (ii), Theorem 2.16, page 49 of [6] to get

$$(36) \quad \|\omega_{\tilde{\beta}}(x) - \omega_{\beta}(x)\| \leq \frac{|\beta - \tilde{\beta}|}{|\tilde{\beta}|} \|\omega_{\beta}\|$$

with the true solution ω of $\mathbb{F}\omega = u^{\infty}$. Since $\omega_{\beta} \rightarrow \omega$ for $\beta \rightarrow 0$ we obtain (32).

We now consider the case where $\beta = K\overline{\gamma}_m\gamma_m\alpha$. Using the same computation procedure as given in the proof of Theorem 3.3, we get that

$$(37) \quad \begin{aligned} & \gamma_m(u_{\alpha}^s(x) - v_{\beta}^s(x)) \\ &= \sum_{j,l \in \mathbb{N}} \frac{\mu_l}{\alpha + \mu_j^2} \langle \psi, \psi_j \rangle_{L^2(\partial G)} \langle \varphi, \varphi_l \rangle_{L^2(\mathbb{S}^{m-1})} \langle \psi_l, \overline{\psi_j} \rangle_{L^2(\partial G)} \\ & \quad - \sum_{j,l \in \mathbb{N}} \frac{\mu_l}{K\alpha + \mu_l^2} \langle \psi, \psi_j \rangle_{L^2(\partial G)} \langle \varphi, \varphi_l \rangle_{L^2(\mathbb{S}^{m-1})} \langle \psi_l, \overline{\psi_j} \rangle_{L^2(\partial G)}. \end{aligned}$$

It follows from Lemma 3.1 that $\langle \psi_l, \overline{\psi_j} \rangle_{L^2(\partial G)} = 0$ for $\mu_l \neq \mu_j$. Therefore (37) becomes

$$(38) \quad \begin{aligned} & u_{\alpha}^s(x) - v_{\beta}^s(x) \\ &= (K-1) \gamma_m^{-1} \sum_{j,l \in \mathbb{N}, \mu_l = \mu_j} \frac{\alpha \mu_j}{(\alpha + \mu_j^2)(K\alpha + \mu_j^2)} \langle u^{\infty}, \varphi_l \rangle \langle \Phi(\cdot, x), \psi_j \rangle \langle \psi_l, \overline{\psi_j} \rangle \\ &= \frac{(K-1)}{K} \gamma_m^{-1} \sum_{j,l \in \mathbb{N}, \mu_l = \mu_j} \frac{\mu_j}{(\alpha + \mu_j^2)} \frac{K\alpha}{(K\alpha + \mu_j^2)} \langle u^{\infty}, \varphi_l \rangle \langle \psi_l, \overline{\psi_j} \rangle \langle \Phi(\cdot, x), \psi_j \rangle \\ &=: \frac{(K-1)}{K} \omega(K, \alpha), \end{aligned}$$

where $\omega(K, \alpha)$ is given by the series in (38). It is readily seen to be well-defined and convergent by comparison with (29), from which it differs by the bounded factor

$$(39) \quad r(\alpha, \mu) := \frac{K\alpha}{(K\alpha + \mu^2)}, \quad |r(\alpha, \mu)| < 1, \quad |r(\alpha, \mu)| \rightarrow 0, \quad \alpha \rightarrow 0$$

for fixed $\mu > 0$. Following standard arguments for the convergence of the Tikhonov regularization it is seen that $\omega(K, \alpha) \rightarrow 0, \alpha \rightarrow 0$ for any fixed K , which is in fact uniform for $K \geq K_0$ for any $K_0 > 0$. Alternatively, we can argue

$$(40) \quad \frac{|K-1|}{K} |\omega(K, \alpha)| \leq |u_\alpha^s(x) - u(x)| + |v_\beta^s(x) - u(x)|.$$

Since $u_\alpha^s(x), v_\beta^s(x)$ are the Tikhonov regularizing solution to $u(x)$ given by Algorithm 2.1 and Algorithm 2.2 respectively, then we get

$$|u_\alpha^s(x) - u(x)|, |v_\beta^s(x) - u(x)| \rightarrow 0 \quad \text{as } \alpha \rightarrow 0,$$

noticing $\beta = K\bar{\gamma}_m\gamma_m\alpha \rightarrow 0$. That is, $\omega(K, \alpha) \rightarrow 0$ as $\alpha \rightarrow 0$ from (40). The proof is complete. \square

This theorem reveals the quantitative relation of two reconstruction algorithms, namely, it gives the difference of the error for these two regularizing schemes. The factor $K-1$ indicates the coupling relation of these two schemes in terms of the constant K , while $\omega(K, \alpha)$ represents the regularizing property of these two schemes. More precisely, we conclude for $\beta = K\bar{\gamma}_m\gamma_m\alpha$ that $|u_\alpha^s(x) - u(x)| \rightarrow |v_\beta^s(x) - u(x)|$ either as $K \rightarrow 1$ for any fixed $\alpha > 0$ or as $\alpha \rightarrow 0$ for any fixed $K > 0$.

4. Numerical tests. In this final section we study numerical implementations of computing the scattered wave from its far-field pattern, using point source method and potential method respectively. Notice, the *golden rule* for the regularizing parameters of these two schemes is independent of the boundary type of the obstacle and true for 2-dimensional and 3-dimensional obstacles.

Example 1. Consider the following 2-dimensional problem. For a given obstacle $D \subset \mathbb{R}^2$ and given incident wave $u^i(x)$, the scattered wave $u^s(x)$ outside of \bar{D} is governed by

$$(41) \quad \begin{cases} \Delta u^s + \kappa^2 u^s = 0, & x \in \mathbb{R}^2 \setminus \bar{D} \\ \mathcal{B}u^s = -\mathcal{B}u^i, & x \in \partial D \\ \frac{\partial u^s}{\partial r}(x) - i\kappa u^s(x) = o\left(\frac{1}{\sqrt{r}}\right), & r = |x| \rightarrow \infty \end{cases}$$

where \mathcal{B} is the boundary operator which represents the acoustic property of the obstacle such as sound-soft, sound-hard or impedance boundary condition.

Firstly, we take point incident wave $u^i(x) = H_0^{(1)}(\kappa|x - x_0|)$ with $x_0 \in D \subset \mathbb{R}^2$. Then it is easy to see that the scattered wave $u^s(x)$ as well as its far-field pattern has the exact expression

$$(42) \quad u^s(x) = -H_0^{(1)}(\kappa|x - x_0|), \quad x \in \mathbb{R}^2 \setminus \overline{D}$$

and

$$(43) \quad u^\infty(\hat{x}) = \gamma_2 4i e^{-i\kappa\hat{x}\cdot x_0}, \quad \hat{x} \in \mathbb{S}^1.$$

Notice, these two expressions are independent of ∂D and the boundary operator \mathcal{B} for this special incident wave with $x_0 \in D$. That is, we do not need to specify ∂D as well as \mathcal{B} and simulate the far-field pattern by solving the direct problem in this special case.

We take $\kappa = 1.2$, $x_0 = (-0.4, 0.2)$ and the domain G with the boundary

$$\partial G = \{x(t) = (\cos t + 0.65 \cos 2t - 0.65, 1.5 \sin t), t \in [0, 2\pi]\}$$

where we introduce the density functions for two reconstruction schemes, respectively. Then we can compute the scattered wave outside of G . In our numerics, we approximate $u^s(x)$ on

$$\partial G_s := \{x(t) := (3 \cos t, 4.5 \sin t), t \in [0, 2\pi]\}$$

by two schemes from the far-field data given by (43). In the computation, we divide the interval $[0, 2\pi]$ into $2n$ subintervals with grids $t_j = \frac{\pi}{n}j : j = 0, 1, \dots, 2n - 1$. The numerical comparison of $u_\alpha^s(x), v_\beta^s(x)$ for β, α satisfying the *golden rule* $\beta = \overline{\gamma}_2 \gamma_2 \alpha$ are listed in the following table for different n at points $t = \pi/2, \pi, 3\pi/2$, where we take $\alpha = 0.0002$, while $u^s(x)$ represents the exact scattered wave given by (42). It can be seen from this table that, for large n the two regularizing schemes with their regularizing parameters meeting the *golden rule* generate the same scattered wave up the accuracy of 10^{-7} , which supports our theoretical analysis.

n		$t = \frac{\pi}{2}$	$t = \pi$	$t = \frac{3}{2}\pi$
	u^s	(0.1163657,0.3297931)	(0.3006898,-0.3327909)	(-4.6991613E-02,0.3314249)
8	u_α^s	(0.1163359,0.3298757)	(0.3007150,-0.3340268)	(-4.7064792E-02,0.3315395)
8	v_β^s	(0.1163362,0.3298748)	(0.3007154,-0.3340252)	(-4.7064558E-02,0.3315395)
16	u_α^s	(0.1163383,0.3298783)	(0.3007144,-0.3339863)	(-4.7057118E-02,0.3315282)
16	v_β^s	(0.1163391,0.3298775)	(0.3007144,-0.3339843)	(-4.7057025E-02,0.3315281)
32	u_α^s	(0.1163383,0.3298784)	(0.3007144,-0.3339867)	(-4.7057308E-02,0.3315285)
32	v_β^s	(0.1163390,0.3298775)	(0.3007144,-0.3339846)	(-4.7057088E-02,0.3315282)
64	u_α^s	(0.1163383,0.3298783)	(0.3007145,-0.3339868)	(-4.7057085E-02,0.3315282)
64	v_β^s	(0.1163386,0.3298782)	(0.3007145,-0.3339871)	(-4.7057357E-02,0.3315287)

Table 1: A comparison of u_α^s, v_β^s and exact u^s at different points.

Now let us check these two reconstruction for regularizing parameters not satisfying the "golden rule". If we take $\beta = K\overline{\gamma}_m\gamma_m\alpha$ with different K , compare the reconstruction of these two schemes. In this test, we fix $n = 32$ and compute the scattered waves by the two schemes for this scattering model with exact $u^s(x)$ expression. The errors of $\log |(v_\beta^s - u_\alpha^s)(x(t))|$ and $\log |(v_\beta^s - u^s)(x(t))|$ in $t \in [0, 2\pi]$ for fixed small $\alpha = 10^{-3}$ and different $K = 2, 1.2, 1.0, 0.5, 0.1$ are shown in Figure 1.

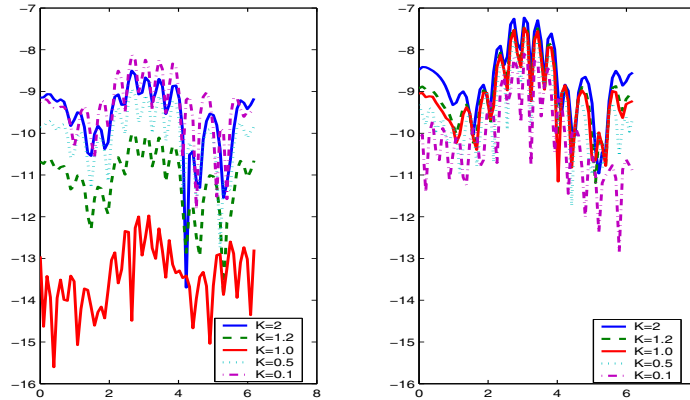


Figure 1: Comparison of $v_\beta^s - u_\alpha^s$ and $v_\beta^s - u^s$ for different K .

It can be seen from this figure that, the error $|(v_\beta^s - u^s)(x(t))|$ becomes small as K decreases (right figure), which means $v_\beta^s(x) \rightarrow u^s(x)$ as $\beta \rightarrow 0$, noticing that we take $\beta = K\overline{\gamma}_2\gamma_2\alpha$ for fixed α . However,

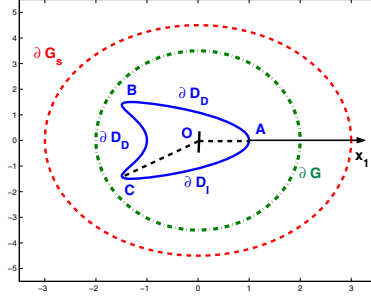


Figure 2: Configuration of the non-convex obstacle with mixed boundary condition.

the minimum value $(v_\beta^s - u_\alpha^s)(x(t))$, which represents the error of two regularizing schemes, always appears for $K = 1$ (left figure), which supports our theoretical analysis given by Theorem 3.5.

Example 2. Next, consider the reconstruction of scattered wave for an incident plane wave. We need to simulate the far-field pattern by solving direct problem, since no exact solution is available in this case. So we specify the obstacle D with the boundary

$$\partial D = \{x(t) = (\cos t + 0.65 \cos 2t - 0.65, 1.5 \sin t), t \in [0, 2\pi]\}$$

on which the mixed boundary condition is assumed by defining

$$\mathcal{B} := \begin{cases} \mathcal{I}, & x(t) \in \widehat{ABC} \subset \partial D \quad \text{with } t \in [0, 1.42\pi] \\ \frac{\partial}{\partial \nu} + 3i\kappa, & x(t) \in \widehat{CA} \subset \partial D \quad \text{with } t \in (1.42\pi, 2\pi]. \end{cases}$$

In the computation, we introduce the density functions in

$$\partial G := \{x(t) = (2 \cos t, 3.5 \sin t), t \in [0, 2\pi]\}$$

and compute the scattered wave on

$$\partial G_s := \{x(t) = (3 \cos t, 4.5 \sin t), t \in [0, 2\pi]\},$$

see Figure 2 for the configuration.

n		$t = \frac{\pi}{2}$	$t = \pi$	$t = \frac{3}{2}\pi$
8	u_α^s	(4.7237091E-02,0.6326757)	(-0.4285755,-0.4107293)	(7.5148039E-02,-0.2332105)
8	v_β^s	(4.7241095E-02,0.6326982)	(-0.4285603,-0.4107074)	(7.5148977E-02,-0.2332066)
16	u_α^s	(4.9253341E-02,0.6331174)	(-0.4171216,-0.4172901)	(8.1694886E-02,-0.2209388)
16	v_β^s	(4.9250260E-02,0.6331332)	(-0.4171319,-0.4172804)	(8.1686519E-02,-0.2209338)
32	u_α^s	(4.9657788E-02,0.6336886)	(-0.4252205,-0.4166148)	(8.3241701E-02,-0.2297525)
32	v_β^s	(4.9668275E-02,0.6336918)	(-0.4252321,-0.4166267)	(8.3240218E-02,-0.2297502)
64	u_α^s	(5.0019212E-02,0.6338249)	(-0.4233266,-0.4170950)	(8.4115691E-02,-0.2269450)
64	v_β^s	(5.0033569E-02,0.6338263)	(-0.4233316,-0.4171042)	(8.4116094E-02,-0.2269421)

Table 2: A comparison of u_α^s, v_β^s for plane wave with incident direction $d = (0.6, 0.8)$.

For $K = 1, \alpha = 0.0002$, the reconstruction results by these two schemes evaluated for three different points are listed in the table, while the error distribution of

$$|\operatorname{Re}(u_\alpha^s - v_\beta^s)(x(t))|$$

and

$$|\operatorname{Im}(u_\alpha^s - v_\beta^s)(x(t))|$$

on ∂G_s are shown in Figure 3 by a polar coordinate system. We can also see that in this non-convex obstacle case, the two schemes generate the same results for their regularizing parameters satisfying the *golden rule*. Here, the accuracy is less than in Example 1 due to the more complex field for the scattering process of an obstacle with mixed boundary condition.

Conclusion. In this paper, we compare two well known regularizing schemes of reconstructing the scattered wave from its far field pattern

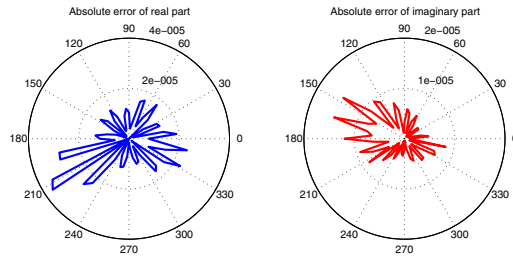


Figure 3: Error distribution of $|\Re(v_\beta^s - u_\alpha^s)(x(t))|$ and $|\Im(v_\beta^s - u_\alpha^s)(x(t))|$.

from a quantitative point of view. The main step in these two inversion schemes is to solve an integral equation of the first kind with respect to the density function from which the scattered wave is approximated. We establish a *golden rule* for the regularizing parameters of these two schemes. This new quantitative relation between these two schemes, together with the derivation procedure introduced in the previous paper [8], reveals the fundamental relation of these two schemes. Roughly speaking, these two schemes are equivalent in the sense of their dual relation and their quantitative uniformness for regularizing parameters satisfying the *golden rule*, providing identical reconstructions when the geometrical setting is chosen adequately.

Acknowledgement. This work is supported by NSFC (No.10371018). The first author thanks the hospitality of Institute of Numerical and Applied Mathematics at University of Göttingen during his visit in the winter of 2006.

REFERENCES

1. J. Cheng, J. J. Liu and G. Nakamura, *Recovery of boundaries and types for multiple obstacles from the far-field pattern*, to appear in Quart. Applied Maths.
2. ———, *The numerical realization of the probe method for the inverse scattering problems from the near field data*, Inverse Problems, Vol. **21**, No.3, (2005), 839–855.
3. D. L. Colton and A. Kirsch, *A simple method for solving inverse scattering problems in the resonance region*, Inverse Problems, Vol. **12**, (1996), 383–393.
4. D. L. Colton and R. Kress, *Inverse Acoustic and Electromagnetic Scattering Theory*, 2nd edition, Springer-Verlag, Berlin, (1998).
5. K. Erhard, *Point Source Approximation Methods in Inverse Obstacle Reconstruction Problems*, Dissertation Thesis, Göttingen (2005).
6. A. Kirsch, *An Introduction to the Mathematical Theory of Inverse Problems*, Springer Verlag (1996).
7. R. Kress, *Linear Integral Equations*, Springer Verlag, (1989).
8. J. J. Liu, G. Nakamura and R. Potthast, *A new approach and improved error analysis for reconstructing the scattered wave by the point source method*, J. Comput. Maths, Vol. **25**, No.2, (2007), 113–130.
9. R. Potthast, *Point sources and multipoles in inverse scattering theory*, Chapman & Hall/CRC Research Notes in Mathematics, Chapman & Hall/CRC, Boca Raton, FL, Vol. **427**, (2001).

10. ———, *Stability estimates and reconstructions in inverse acoustic scattering using point sources*, J. Appl. Comput. Maths, Vol. **114**, No.2, (2000), 247–274.

11. ———, *Topical Review: A survey on sampling and probe methods for inverse problems*, Inverse Problems, Vol. **22**, R1-R47, (2006).

12. ———, *A point-source method for inverse acoustic and electromagnetic obstacle scattering problems*, IMA J. Appl. Maths., Vol. **61**, (1998), 119-140.

13. ———, *Sampling and Probe Methods - An Algorithmical View*, Computing, Vol. **75**, (2005), 215-236.

DEPARTMENT OF MATHEMATICS, SOUTHEAST UNIVERSITY, NANJING, 210096,
P.R.CHINA.

Email address: jjliu@seu.edu.cn

UNIVERSITY OF READING, DEPARTMENT OF MATHEMATICS, WHITEKNIGHTS, PO
Box 220, BERKSHIRE, RG6 6AX, UK.

Email address: r.w.e.potthast@reading.ac.uk